fermentation

MDPI

Article

Cell Wall Glycan Changes in Different Brachypodium Tissues Give Insights into Monocot Biomass

Utku Avci

Department of Agricultural Biotechnology, Faculty of Agriculture, Eskisehir Osmangazi University, Eskisehir 26160, Turkey; utkuavci@gmail.com

Abstract: The annual temperate grass *Brachypodium distachyon* has become a model system for monocot biomass crops and for understanding lignocellulosic recalcitrance to employ better saccharification and fermentation approaches. It is a monocot plant used to study the grass cell walls that differ from the cell walls of dicot plants such as the eudicot model Arabidopsis. The *B. distachyon* cell wall is predominantly composed of cellulose, arabinoxylans, and mixed-linkage glucans, and it resembles the cell walls of other field grasses. It has a vascular bundle anatomy similar to C3 grasses. These features make Brachypodium an ideal model to study cell walls. Cell walls are composed of polymers with complex structures that vary between cell types and at different developmental stages. Antibodies that recognize specific cell wall components are currently one of the most effective and specific molecular probes to determine the location and distribution of polymers in plant cell walls in situ. Here, we investigated the glycan distribution in the cell walls of the root and leaf tissues of Brachypodium by employing cell-wall-directed antibodies against diverse glycan epitopes. There are distinct differences in the presence of the epitopes between the root and leaf tissues as well as in the cell type level, which gives insights into monocot biomass.

Keywords: antibody; *Brachypodium distachyon*; cell wall; imaging; microscopy

check for updates

Citation: Avci, U. Cell Wall Glycan Changes in Different Brachypodium Tissues Give Insights into Monocot Biomass. *Fermentation* **2023**, *9*, 52. https://doi.org/10.3390/fermentation9010052

Academic Editor: Liqun Jiang

Received: 25 November 2022
Revised: 26 December 2022
Accepted: 5 January 2023
Published: 8 January 2023

1. Introduction

Climate change and the ever-growing world population necessitates alternatives to fossil-feedstock-based products. Renewable biomass has the potential to create a biobased economy that utilize biorefineries for complete valorization of biomass. Lignocellulosic biomass is an attractive feedstock for the production of biofuels and value-added bioproducts. However, the saccharification and fermentation of biomass requires a high cost, mainly due to lignocellulosic recalcitrance [1]. Additionally, biorefineries are currently far from achieving total biomass valorization. Cellulose, hemicellulose, and lignin as the main constituents of lignocellulosic biomass should be effectively separated and used in product diversification for bioproduct production. Commercialization of each component of biomass canhelp reduce costs. Furthermore, in order to produce valuable and competitive bioproducts from biomass, it is important to better understand plant cell walls to come up with effective biomass deconstruction technologies, which help to reduce the costs of the energy-demanding pretreatments and enzymes used in these processes.

The synthesis and deposition of cell wall glycans to generate cell walls are important features of plant cells. Cell walls, mainly determining the shape and size of plant cells, are predominantly composed of complex carbohydrates. Cellulosic and hemicellulosic polysaccharides bring about a meshwork of polysaccharides that are vital in many mechanisms for plant development and survival [2].

The annual temperate grass *Brachypodium distachyon* has become a model system for monocot biomass crops and for understanding lignocellulosic recalcitrance to employ better saccharification and fermentation [3–5]. Cell wall composition of Brachypodium has been documented, and organ-specific cell wall chemical compositions have been observed to be

similar to other C3 forage grasses [6,7]. These studies tell us about the overall makeup of the cell wall composition, but they stay short in terms of where in the plant these cell wall components are localized. Immunohistochemical studies are vital to fill this gap. There are a limited number of studies where cell-wall-directed antibodies are used in Brachypodium. The spatial and temporal distribution of the cell wall glycans were detected during the grain development of *Brachypodium distachyon* [8]. The distribution of arabinogalactan proteins, extensins, pectins, and hemicelluloses are localized in the developing embryo [9] and in the embryogenic callus cells of Brachypodium [10,11]. However, to our knowledge, there are no studies depicting localization of cell wall glycans in the root and leaves of Brachypodium in detail.

Grasses have many cell wall features that are distinct from eudicots and other plants [12]. The *B. distachyon* cell wall is predominantly composed of cellulose, mixed linkage glucans [(1,3;1,4)-β-D-glucans], and arabinoxylans. The molecular structures of most cell wall glycans are known; however, there is still limited knowledge about how these polysaccharides are orchestrated in different tissues or cells to bring about unique cell walls. Such information could facilitate the better understanding of cell wall machinery and the development of effective techniques to utilize grass biomass sources.

Here, we investigated the distribution of various cell wall glycans in two different tissues of Brachypodium by employing a set of cell-wall-directed monoclonal antibodies against hemicellulose, pectin, mixed-linkage glucan, and arabinogalactan proteins for the first time. Distinct localization patterns and differences in the root and leaf imply different utilization of cell wall glycans in different cells and tissues. Such information could be valuable for saccharification and fermentation processes depending on the biomass source used.

2. Materials and Methods

2.1. Plant Growth and Tissue Processing

The diploid inbreed *Brachypodium distachyon* line Bd21 was used. After peeling off the lemma of mature seeds, sterilization was started in 70% ethanol (*v*/*v*) for 2 min. After ethanol treatment, the seeds were soaked in 1% sodium hypochlorite (*v*/*v*) for 5 min and rinsed with sterile deionized water three times. The seeds were then placed on square plates with growth media containing half-strength Murashige-Skoog (MS) (2.45 g/L MS salts with vitamins, 1% sucrose, 1% agar, and pH 5.7). The plates were stratified for 2 days at 4 °C and transferred to a growth chamber under continuous light of 100–120 µE intensity at 22 °C. The root and leaf tissues were harvested with a sharp razor blade from 10-day-old (days after germination) plantlets. The tissues were fixed and processed for immunolabeling as described [13].

2.2. Ultramicrotomy and Immmunolabeling

250 nm-thick cross-sections from the root and leaf tissue blocks were cut by a Leica UC7 ultramicrotome (Leica, Vienna, Austria) and mounted on ColorFrost Plus glass slides (Thermo Fisher Scientific, Waltham, MA, USA). Immunolabeling was carried out as described in detail [13]. As a secondary antibody, an Alexa fluor 488 goat anti-rat was used for the LM series of antibodies and an Alexa fluor 488 goat anti-mouse was used for the CCRC series of antibodies. All of the antibodies used in this study did not show any unspecific binding. Approximately 200 wall-directed monoclonal antibodies have been produced over the years in different laboratories. These monoclonal antibodies are available and they specifically recognize glycan epitopes on xyloglucan, xylan, mannan, arabinogalactan, homogalacturonan, or rhamnogalacturonan I [14,15]. These antibodies were obtained from stock centers (CarboSource Services, CCRC, University of Georgia, USA (https://carbosource.uga.edu/, accessed on 20 November 2022); Biosupplies, Australia (http://www.biosupplies.com.au, accessed on 20 November 2022). Separate sections of each tissue were stained with toluidine blue (0.05% *w*/*v* in water) to observe the plant's anatomy under light microscopy. Images were captured on a Zeiss Axio Imager M2 mi-

croscope (Carl Zeiss, Jena, Germany) with epifluorescence optics and a digital camera (Axiocam 503, Carl Zeiss, Jena, Germany). The exposure times were kept constant for each antibody result from both the root and leaf tissues to allow for equal comparison. The images were assembled using Adobe Photoshop (Adobe Systems, San Jose, CA, USA).

3. Results

The general anatomy of the Brachypodium root and leaf is shown in toluidine-blue-stained sections (Figure 1). In the root sections, the root hairs, epidermis, cortex cells, endodermis, and vascular cells can be observed (Figure 1A, arrows). In the leaf sections, the upper and lower epidermis, mesophyll cells, bulliform cells, sclerenchyma cells, trichome, phloem, and xylem cells can be seen (Figure 1B, arrows). Following this, immunolabeling experiments were carried out on consecutive sections taken from the same areas.

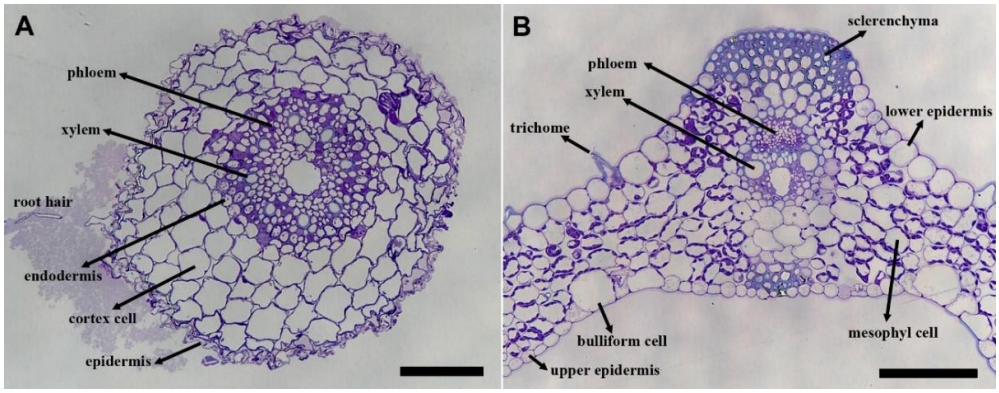

Figure 1. Toluidine-blue-stained sections of the Brachypodium root (**A**) and leaf (**B**). The general anatomical features of the root and leaf are shown. Arrows indicate the cell types in the root (root hair, epidermis, cortex cells, endodermis, xylem, and phloem) and leaf section (upper epidermis, lower epidermis, trichome, bulliform, mesophyll, sclerenchyma, xylem, and phloem). Immunolabeling was carried out on consecutive sections. The scale bar is equal to 25 μm in both images.

Immunolabeling

Figure 2 shows the localization of four xylan-directed monoclonal antibodies that recognize different epitopes on the xylan. Since the xylan is decorated with various substitutions, it is important to visualize the different decorations by using specific antibodies. CCRC-M148 only binds to the linear unbranched xylan backbone with a degree of polymerization (DP) of six or more [16]. It does not tolerate any substitution. In the root, weaker labeling is observed in the cortex cells compared to those in the epidermal cells and the cells in the stele (Figure 2A) with CCRC-M148. In the leaf, the sclerenchyma cells and vascular cells are strongly labeled by CCRC-148 (Figure 2B). These results suggest that epidermal cells and cells in the stele such as vascular cells (xylem and phloem) have more unbranched xylan (DP six or more) compared to the cortex cells in the root and mesophyll cells in the leaf. CCRC-M154 binds specifically to arabinosyl-substituted xylans, namely arabinoxylans [16]. This antibody labeled all of the cell walls ubiquitously in the root and leaf (Figure 2C,D), indicating the arabinoxylan is present in all of the cell walls. LM10 binds to the non-reducing end of xylans [17] whereas LM11 binds to the xylan backbone with a high tolerance for substitution [17]. The LM10 and LM11 labeling in the leaf tissue were similar whereas LM11 labeled the root tissue more strongly (Figure 2E–H). Stronger labeling in the root with LM11 indicates there is more substitution on the xylan backbone in this tissue compared to that in the leaf. The leaf trichome cells were also labeled by four xylan antibodies (Figure 2B,D,F,H).

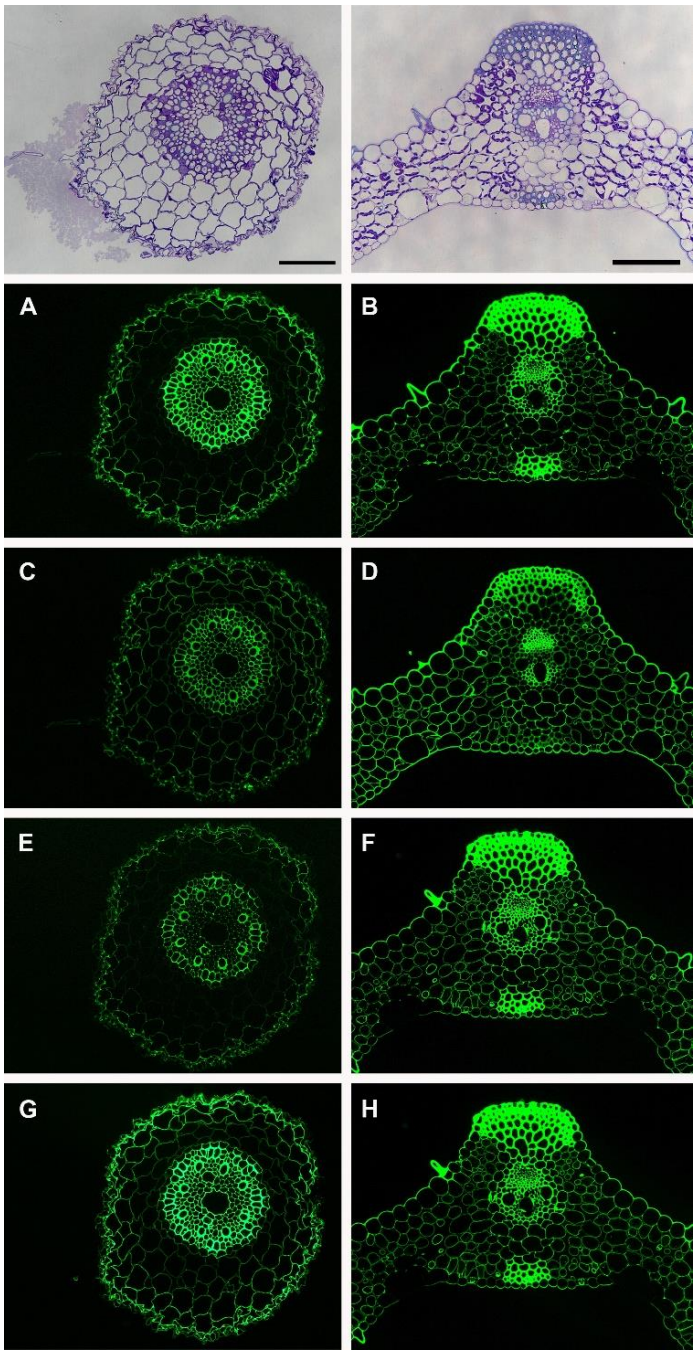

Figure 2. Immunolabeling of the Brachypodium root and leaf with xylan-directed antibodies; CCRC-M148 (**A**,**B**), CCRC-M154 (**C**,**D**), LM10 (**E**,**F**), and LM11 (**G**,**H**). The scale bars are equal to 25 µm and apply to the immunolabeling images for each tissue.

Pectic glycans are mainly composed of homogalacturonans (HGs) and rhamnogalacturonans. HGs are deposited in the cell walls in a highly methyl-esterified form and LM19 and LM20 antibodies can differentiate methyl esterification patterns where LM19 binds to unesterified HGs and LM20 binds to esterified HGs [18]. LM19 did not show labeling in both tissues (Figure 3A,B) whereas LM20 labeled the cell corners in the leaf tissue (Figure 3C,D), which indicates that the leaf tissue has more methyl esterification than the roots. The motifs on pectic polymer rhamnogalacturonan-I (RG-I) can be detected by LM5 for 1,4-galactan and LM6 for 1,5-arabinan even though the same epitopes can be found in arabinogalactan proteins (AGPs) since rhamnogalacturonan and AGPs have similar decorations. LM5 labeling was weak both in the root and leaf (Figure 3E,F). In the root, the

labeling was more apparent in epidermal and cortex cells with a lower fluorescent signal. In the leaf, the labeling was restricted to the trichome and sclerenchyma cells. These results with LM5 indicate the presence of 1,4-galactan in the epidermis and cortex cells in the root and sclerenchyma and trichome cells in the leaf. On the other hand, LM6 labeling was strong and it labeled all of the cell walls in both tissues (Figure 3G,H), which indicates that there is the presence of 1,5-arabinan in all of the cell walls. Punctate labeling was also observed inside the cells adjacent to the cell walls (Figure 3G,H) which might be due to the binding of the LM6 antibody to the 1,5-arabinan epitopes found in AGP [19].

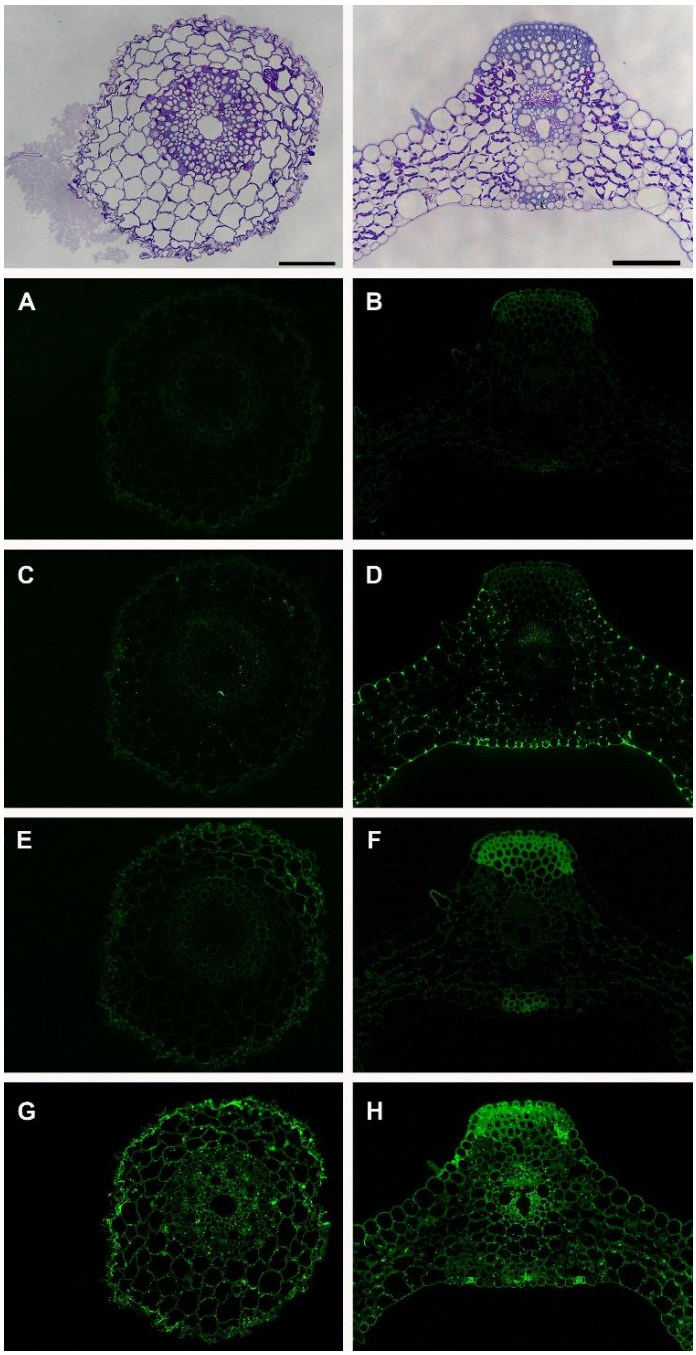

Figure 3. Immunolabeling of the Brachypodium root and leaf with pectin-directed antibodies; LM19 (**A**,**B**), LM20 (**C**,**D**), LM5 (**E**,**F**), and LM6 (**G**,**H**). Scale bars equal to 25 µm and apply to immunolabeling images for each tissue.

CCRC-M1 recognizes fucosylated xyloglucan [20] and LM15 recognizes the XXXG-motif of xyloglucan [21]. CCRC-M1 did not show any labeling in both tissues (Figure 4A,B), indicating that the fucose residue on the xyloglucan was not available to the antibody. LM15 labeling was stronger in the epidermal cells in the root (Figure 4C) whereas it only labeled sclerenchyma cells in the leaf tissues (Figure 4D), which implies that the XXXG motif of xyloglucan is localized in different cell types in the root and leaf tissues. CCRC-M82 recognizes AGPs [15]. It showed stronger labeling in the epidermal cells of the root (Figure 4E) and punctate labeling in both the root and leaf (Figure 4E,F). The BG1 antibody recognizes (1,3; 1,4)-β-$_D$-glucan, namely mixed linkage glucans [22]. In the root, BG1 labeled epidermal cells and the cells in the stele (Figure 4G). In the leaf, BG1 labeled epidermal cells, sclerenchyma cells, and vascular cells (Figure 4H) where the labeling was stronger than that in the root. The cortex cells in the root and the mesophyll cells in the leaf did not show the presence of MLG epitopes, which indicated the differential synthesis of MLG in the different cell types.

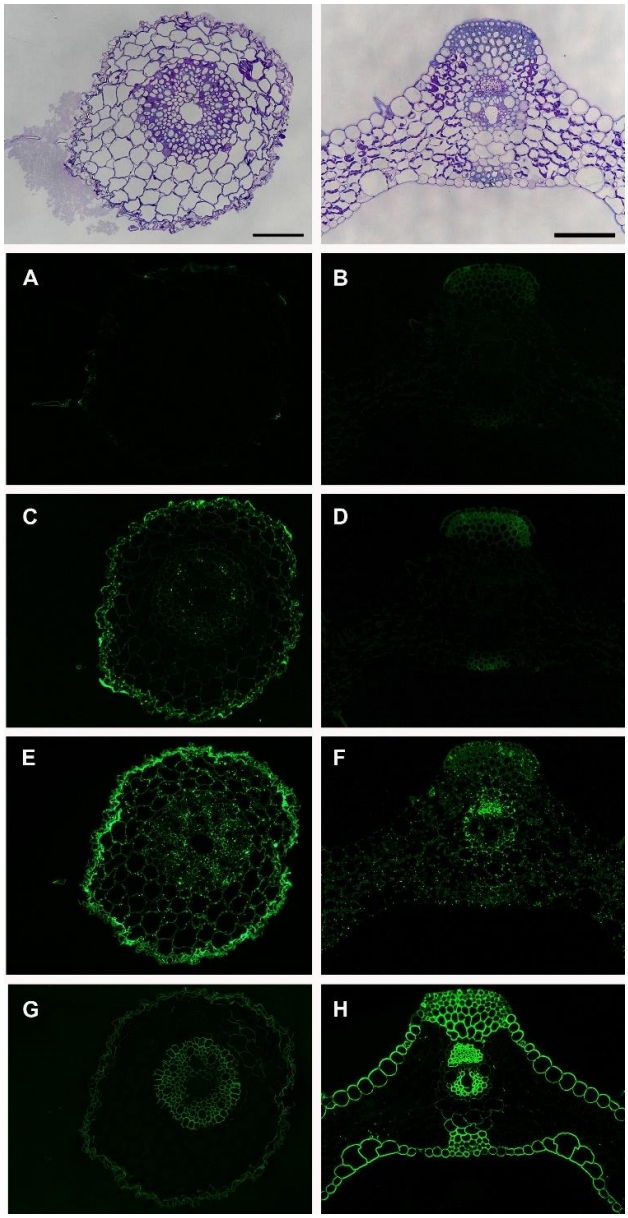

Figure 4. Immunolabeling of the Brachypodium root and leaf with xyloglucan, arabinogalactan, and mixed-linkage glucan antibodies; CCRC-M1 (**A**,**B**), LM15 (**C**,**D**), CCRC-M82 (**E**,**F**), and BG1 (**G**,**H**). The scale bar is equal to 25 μm and applies to the immunolabeling images for each tissue.

4. Discussion and Conclusions

The global supply of fossil-based fuels is diminishing. On the other hand, with the ever-growing world population, the energy demand is increasing. When climate change and increasing prosperity are added, it becomes obvious that there needs to be a transition from fossil-based fuels and products to more sustainable and renewable sources. Lignocellulosic biomass is a renewable source and has a big potential to make this transition. Plants capture carbon dioxide and synthesize polymers. For example, cellulose is one of the most important and abundant renewable polymer and it is deposited in plant cell walls.

Plant cell wall biopolymers have complex and dynamic structures. The components of cell walls crosslink with each other and create nanoscale architectures that can show changes from one plant species to other and also in different organs or tissues of the same plant. Such changes define the shape and role of each cell. Cell wall polymers are also dynamic components and can be restructured during development and in response to biotic and abiotic stresses. A Better understanding of plant cell walls can help us design biomass feedstocks that could be efficiently used in biorefineries.

Brachypodium distachyon has a sequenced genome; genetic transformations protocols have been established and mutant collections are available [23]. Therefore, it has become a model system for monocot biomass crops. It is also valuable for understanding lignocellulosic recalcitrance to employ better saccharification and fermentation approaches. For example, cell wall composition and biomass recalcitrance differences within a genotypically diverse set of *Brachypodium distachyon* inbred lines were studied [4]. Therefore, in similar studies, our results could be used to make comparisons among transgenic and mutant plant lines to assess the presence of cell wall glycans towards a better understanding of cellular mechanisms and changes in biomass stemming from different genotypes. Such approaches could help find less recalcitrant plant lines that would be more favorable for the production of bioproducts.

Similar to other grasses, Brachypodium has a type II wall and based on the biochemical analyses, type II walls differ from those of dicots in terms of the types and abundance of polysaccharides [12,24]. In type II walls, glucuronoarabinoxylans and mixed-linkage glucans are predominant whereas pectin and xyloglucans are present at low levels. Therefore, studies to show the differences among the organs and species of grass cell walls and dicot cell walls will help towards a better understanding of cell wall composition and biosynthesis.

Xylan is one of the major hemicellulosic components of cell walls. In dicots, xylan is predominantly localized in secondary cell walls [15,25]. The major hemicellulose in grasses are heteroxylans, which consist of a (1,4)-β-d-xylopyranosyl backbone, bearing side chains of arabinose, xylose, and glucuronic acid [26]. Grass cell walls have an abundance of arabinoxylans and glucuronoarabinoxylans compared to the prevalent form of glucuronoxylans in eudicots [26]. Arabinoxylans are found to be one of the main polysaccharides in Brachypodium grains [8]. The 12-day-old seedlings show a similar Ara/Xyl molar ratio (leaves: 0.24 and roots: 0.29) [7]. Our results are consistent with the literature that states that arabinoxylans are ubiquitously distributed in all of the cells of the root and leaf tissues and the intensity of the labeling is similar in both tissues. Stronger labeling with the LM10 antibody also indicated that the xylan backbone in Brachypodium is highly substituted.

Pectic glycans are present at low levels in type II walls compared to those in the type I walls of dicots [24]. Our results indicated the presence of homogalacturonan in the cell walls of specific cells and the cell corners at low levels. In the Brachypodium embryo, the LM19 antibody that binds to unesterified HGs showed labeling in the seed coat, mesocotyl, and radicula [9]. LM19 and LM20 both labeled the cells in the embryogenic cultures of Brachypodium [10,11]. In our results, LM19 did not show any labeling in the root and leaf whereas LM20, which binds to esterified HGs, showed labeling mainly in the cell corner of the leaf tissue, which implies that the esterified form of HGs is predominant in 10-day-old Brachypodium. This is also consistent with the fact that HGs are deposited in the cell

walls in a highly methyl-esterified form and become de-esterified during development. The results also prove that the esterification of HGs is regulated differently in different tissues. The LM6 antibody showed labeling in the mesocotyl, radicula, and root cap cells of the Brachypodium embryo [9] and embryogenic callus cells [10,11]. Similarly, our results showed labeling of the LM6 antibody in both the root and leaf tissues.

Xyloglucans are also present at low levels in Brachypodium. The CCRC-M1 antibody could not detect any fucosylated xyloglucan whereas the LM15 antibody showed labeling, especially the epidermal cells of the root. A lower labeling pattern is consistent with the literature [24].

Mixed-linkage glucans (MLG) were once thought to be specific to Poaceae; however, later studies have shown its wider distribution in algae, lichens, fungi, and bryophytes [27]. In Brachypodium, CslF6 plays a role in the production of MLGs [28]. Then Golgi-localized synthesis of MLG was shown in maize [29], but there is also evidence that MLG synthesis may occur in the plasma membrane in grasses [30]. A strong fluorescence was observed at the early stages of Brachypodium endosperm development with the MLG-specific antibody [31]. Our results indicate strong labeling in the cell walls of the epidermis and vascular cells in both tissues. However, we did not observe any labeling inside the cells indicating Golgi-derived labeling. Further electron microscopy studies might help to clarify MLG synthesis occurring in the Golgi or plasma membrane in grasses.

Our results are limited by the availability of the range of cell-wall-directed monoclonal antibodies available for our use. Similar studies with other cell-wall-directed antibodies or in different developmental stages and in tissues can reveal more about Brachypodium cell walls. Additionally, efforts to produce more antibodies that can specifically recognize diverse cell wall epitopes that are not covered by the current ones should continue in order to further our understanding about the diversity and the biosynthesis of cell walls. Our results are also based on chemically fixed and processed samples and represent a single shot of each section with each antibody. The production of fluorescently tagged cell wall components could help us to visualize plant cell walls in real time without any disruption. Therefore, research towards such applications with the availability of a higher resolution microscope could further advance our understanding.

The development of redesigned plants or crops with lower recalcitrance by newly available genome editing technologies such as CRISPR would be an important step to maximize biomass utilization. Such approaches require a concrete understanding of the composition and the synthesis of plant cell walls to edit candidate genes in order to reduce recalcitrance and increase biomass. Furthermore, chemists should come up with profitable products and bioprocess engineers should come up with biorefineries that are more cost-saving to operate and could also produce diverse products to fully maximize biomass utilization.

The cell wall proteomes of Brachypodium have been demonstrated for different tissues [32] as well as for plants exposed to different stress conditions [33,34], which resulted into different proteome profiles. Such results hint at the proteins that might be good candidates for genome editing approaches by creating plants with modified cell walls for better utilization in saccharification for bioethanol production or the production for value-added products from biomass. Our results could be used in such studies to observe changes in model plant Brachypodium cell walls for improvement of our understanding towards better utilization of monocot biomass.

Funding: The author thanks TUBITAK (Project No.: 116C063) and Recep Tayyip Erdogan University Scientific Research Projects (BAP) Unit (Project No.: FAP-2016-634) for the funding.

Data Availability Statement: Not applicable.

Acknowledgments: The author would like to thank Michael G. Hahn for supplying the cell-wall-directed monoclonal antibodies.

Conflicts of Interest: The author declares no conflict of interest.

References

1. Liu, Y.; Tang, Y.; Gao, H.; Zhang, W.; Jiang, Y.; Xin, F.; Jiang, M. Challenges and Future Perspectives of Promising Biotechnologies for Lignocellulosic Biorefinery. *Molecules* **2021**, *26*, 5411. [CrossRef] [PubMed]
2. Keegstra, K. Plant cell walls. *Plant Physiol.* **2010**, *154*, 483–486. [CrossRef]
3. Marriott, P.E.; Sibout, R.; Lapierre, C.; Fangel, J.U.; Willats, W.G.T.; Hofte, H.; Gomez, L.D.; McQueen-Mason, S.J. Range of cell-wall alterations enhance saccharification in *Brachypodium distachyon* mutants. *Proc. Natl. Acad. Sci. USA* **2014**, *111*, 14601–14606. [CrossRef] [PubMed]
4. Cass, C.L.; Lavell, A.A.; Santoro, N.; Foster, C.E.; Karlen, S.D.; Smith, R.A.; Ralph, J.; Garvin, D.F.; Sedbrook, J.C. Cell Wall Composition and Biomass Recalcitrance Differences Within a Genotypically Diverse Set of *Brachypodium distachyon* Inbred Lines. *Front. Plant Sci.* **2016**, *7*, 708. [CrossRef] [PubMed]
5. Głazowska, S.; Baldwin, L.; Mravec, J.; Bukh, C.; Hansen, T.H.; Jensen, M.M.; Fangel, J.U.; Willats, W.G.T.; Glasius, M.; Felby, C.; et al. The impact of silicon on cell wall composition and enzymatic saccharification of *Brachypodium distachyon*. *Biotechnol. Biofuels* **2018**, *11*, 171. [CrossRef] [PubMed]
6. Christensen, U.; Alonso-Simon, A.; Scheller, H.V.; Willats, W.G.; Harholt, J. Characterization of the primary cell walls of seedlings of *Brachypodium distachyon*—A potential model plant for temperate grasses. *Phytochemistry* **2010**, *71*, 62–69. [CrossRef]
7. Rancour, D.M.; Marita, J.M.; Hatfield, R.D. Cell wall composition throughout development for the model grass *Brachypodium distachyon*. *Front. Plant Sci.* **2012**, *3*, 266. [CrossRef]
8. Francin-Allami, M.; Alvarado, C.; Daniel, S.; Geairon, A.; Saulnier, L.; Guillon, F. Spatial and temporal distribution of cell wall polysaccharides during grain development of *Brachypodium distachyon*. *Plant Sci.* **2019**, *280*, 367–382. [CrossRef]
9. Betekhtin, A.; Milewska-Hendel, A.; Lusinska, J.; Chajec, L.; Kurczynska, E.; Hasterok, R. Organ and Tissue-Specific Localisation of Selected Cell Wall Epitopes in the Zygotic Embryo of *Brachypodium distachyon*. *Int. J. Mol. Sci.* **2018**, *19*, 725. [CrossRef]
10. Betekhtin, A.; Rojek, M.; Milewska-Hendel, A.; Gawecki, R.; Karcz, J.; Kurczynska, E.; Hasterok, R. Spatial Distribution of Selected Chemical Cell Wall Components in the Embryogenic Callus of *Brachypodium distachyon*. *PLoS ONE* **2016**, *11*, e0167426. [CrossRef]
11. Betekhtin, A.; Rojek, M.; Nowak, K.; Pinski, A.; Milewska-Hendel, A.; Kurczynska, E.; Doonan, J.H.; Hasterok, R. Cell Wall Epitopes and Endoploidy as Reporters of Embryogenic Potential in *Brachypodium distachyon* Callus Culture. *Int. J. Mol. Sci.* **2018**, *19*, 3811. [CrossRef] [PubMed]
12. Carpita, N.C. Structure and biogenesis of the cell walls of grasses. *Annu. Rev. Plant Physiol. Plant Mol. Biol.* **1996**, *47*, 445–476. [CrossRef]
13. Avci, U.; Pattathil, S.; Hahn, M.G. Immunological approaches to plant cell wall and biomass characterization: Immunolocalization of glycan epitopes. In *Biomass Conversion*; Methods in Molecular Biology; Humana Press: Totowa, NJ, USA, 2012; Volume 908, pp. 73–82. [CrossRef]
14. Knox, J.P. Revealing the structural and functional diversity of plant cell walls. *Curr. Opin. Plant Biol.* **2008**, *11*, 308–313. [CrossRef]
15. Pattathil, S.; Avci, U.; Baldwin, D.; Swennes, A.G.; McGill, J.A.; Popper, Z.; Bootten, T.; Albert, A.; Davis, R.H.; Chennareddy, C.; et al. A comprehensive toolkit of plant cell wall glycan-directed monoclonal antibodies. *Plant Physiol.* **2010**, *153*, 514–525. [CrossRef] [PubMed]
16. Schmidt, D.; Schuhmacher, F.; Geissner, A.; Seeberger, P.H.; Pfrengle, F. Automated synthesis of arabinoxylan-oligosaccharides enables characterization of antibodies that recognize plant cell wall glycans. *Chemistry* **2015**, *21*, 5709–5713. [CrossRef] [PubMed]
17. Ruprecht, C.; Bartetzko, M.P.; Senf, D.; Dallabernadina, P.; Boos, I.; Andersen, M.C.F.; Kotake, T.; Knox, J.P.; Hahn, M.G.; Clausen, M.H.; et al. A Synthetic Glycan Microarray Enables Epitope Mapping of Plant Cell Wall Glycan-Directed Antibodies. *Plant Physiol.* **2017**, *175*, 1094–1104. [CrossRef]
18. Verhertbruggen, Y.; Marcus, S.E.; Haeger, A.; Ordaz-Ortiz, J.J.; Knox, J.P. An extended set of monoclonal antibodies to pectic homogalacturonan. *Carbohydr. Res.* **2009**, *344*, 1858–1862. [CrossRef]
19. Willats, W.G.T.; Marcus, S.E.; Knox, J.P. Generation of a monoclonal antibody specific to (1→5)-α-l-arabinan. *Carbohydr. Res.* **1998**, *308*, 149–152. [CrossRef]
20. Puhlmann, J.; Bucheli, E.; Swain, M.J.; Dunning, N.; Albersheim, P.; Darvill, A.G.; Hahn, M.G. Generation of monoclonal antibodies against plant cell-wall polysaccharides. I. Characterization of a monoclonal antibody to a terminal alpha-(1->2)-linked fucosyl-containing epitope. *Plant Physiol.* **1994**, *104*, 699–710. [CrossRef]
21. Marcus, S.E.; Verhertbruggen, Y.; Hervé, C.; Ordaz-Ortiz, J.J.; Farkas, V.; Pedersen, H.L.; Willats, W.G.; Knox, J.P. Pectic homogalacturonan masks abundant sets of xyloglucan epitopes in plant cell walls. *BMC Plant Biol.* **2008**, *8*, 60. [CrossRef]
22. Meikle, P.J.; Hoogenraad, N.J.; Bonig, I.; Clarke, A.E.; Stone, B.A. A (1→3,1→4)-beta-glucan-specific monoclonal antibody and its use in the quantitation and immunocytochemical location of (1→3,1→4)-beta-glucans. *Plant J.* **1994**, *5*, 1–9. [CrossRef]
23. Bragg, J.N.; Wu, J.; Gordon, S.P.; Guttman, M.E.; Thilmony, R.; Lazo, G.R.; Gu, Y.Q.; Vogel, J.P. Generation and characterization of the Western Regional Research Center Brachypodium T-DNA insertional mutant collection. *PLoS ONE* **2012**, *7*, e41916. [CrossRef] [PubMed]
24. Vogel, J. Unique aspects of the grass cell wall. *Curr. Opin. Plant Biol.* **2008**, *11*, 301–307. [CrossRef] [PubMed]
25. McCartney, L.; Marcus, S.E.; Knox, J.P. Monoclonal antibodies to plant cell wall xylans and arabinoxylans. *J. Histochem. Cytochem.* **2005**, *53*, 543–546. [CrossRef]
26. Scheller, H.V.; Ulvskov, P. Hemicelluloses. *Annu. Rev. Plant Biol.* **2010**, *61*, 263–289. [CrossRef]

27. Bulone, V.; Schwerdt, J.G.; Fincher, G.B. Co-evolution of Enzymes Involved in Plant Cell Wall Metabolism in the Grasses. *Front. Plant Sci.* **2019**, *10*, 1009. [CrossRef]
28. Kim, S.J.; Zemelis, S.; Keegstra, K.; Brandizzi, F. The cytoplasmic localization of the catalytic site of CSLF6 supports a channeling model for the biosynthesis of mixed-linkage glucan. *Plant J.* **2015**, *81*, 537–547. [CrossRef] [PubMed]
29. Carpita, N.C.; McCann, M.C. The maize mixed-linkage (1→3),(1→4)-beta-D-glucan polysaccharide is synthesized at the golgi membrane. *Plant Physiol.* **2010**, *153*, 1362–1371. [CrossRef]
30. Wilson, S.M.; Ho, Y.Y.; Lampugnani, E.R.; Van de Meene, A.M.; Bain, M.P.; Bacic, A.; Doblin, M.S. Determining the subcellular location of synthesis and assembly of the cell wall polysaccharide (1,3; 1,4)-β-D-glucan in grasses. *Plant Cell* **2015**, *27*, 754–771. [CrossRef]
31. Guillon, F.; Larré, C.; Petipas, F.; Berger, A.; Moussawi, J.; Rogniaux, H.; Santoni, A.; Saulnier, L.; Jamme, F.; Miquel, M.; et al. A comprehensive overview of grain development in *Brachypodium distachyon* variety Bd21. *J. Exp. Bot.* **2012**, *63*, 739–755. [CrossRef]
32. Douché, T.; Valot, B.; Balliau, T.; San Clemente, H.; Zivy, M.; Jamet, E. Cell wall proteomic datasets of stems and leaves of Brachypodium distachyon. *Data Brief* **2021**, *35*, 106818. [CrossRef] [PubMed]
33. Pinski, A.; Betekhtin, A.; Skupien-Rabian, B.; Jankowska, U.; Jamet, E.; Hasterok, R. Changes in the Cell Wall Proteome of Leaves in Response to High Temperature Stress in *Brachypodium distachyon*. *Int. J. Mol. Sci.* **2021**, *22*, 6750. [CrossRef] [PubMed]
34. Bian, Y.W.; Lv, D.W.; Cheng, Z.W.; Gu, A.Q.; Cao, H.; Yan, Y.M. Integrative proteome analysis of *Brachypodium distachyon* roots and leaves reveals a synergetic responsive network under H_2O_2 stress. *J. Proteom.* **2015**, *128*, 388–402. [CrossRef] [PubMed]